

AD-A170 828

TWO-STAGE FEL (FREE ELECTRON LASER) RESEARCH AT KMS

1/1

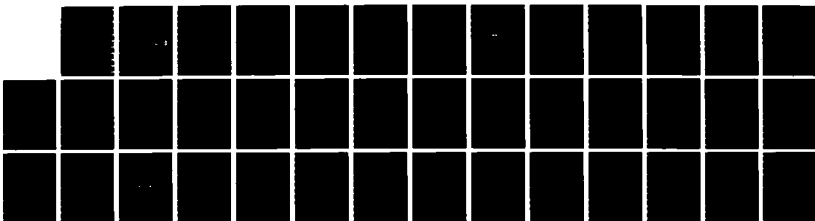
FUSION INC(U) KMS FUSION INC ANN ARBOR MI

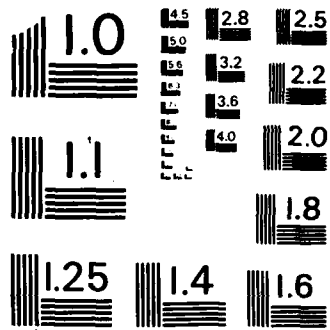
S B SEGALL ET AL. 14 JUL 86. KMSF-U1766 N00014-85-C-0278

UNCLASSIFIED

F78 20/5

NL





MICROCOPY RESOLUTION TEST CHART
NATIONAL BUREAU OF STANDARDS - 1963 - A

12

AD-A170 828

REPORT DOCUMENTATION PAGE		READ INSTRUCTIONS BEFORE COMPLETING FORM
1. REPORT NUMBER KMSF U1766	2. GOVT ACCESSION NO.	3. RECIPIENT'S CATALOG NUMBER
4. TITLE (and Subtitle) Final Report on Two-stage FEL Research at KMS Fusion, Inc.		5. TYPE OF REPORT & PERIOD COVERED Final Report
		6. PERFORMING ORG. REPORT NUMBER
7. AUTHOR(s) Stephen B. Segall, S. Von Laven, M. S. Curtin, P. Diament, J. F. Ward, and P. Farrell		8. CONTRACT OR GRANT NUMBER(s) N00014-85-C-0278
9. PERFORMING ORGANIZATION NAME AND ADDRESS KMS Fusion, Inc. 3621 South State Rd., P.O. Box 1567 Ann Arbor, MI 48106		10. PROGRAM ELEMENT, PROJECT, TASK AREA & WORK UNIT NUMBERS
11. CONTROLLING OFFICE NAME AND ADDRESS Defense Contract Administration Services Management Area, Detroit McNamara Federal Building, 477 Michigan Avenue Detroit, MI 48226		12. REPORT DATE July 14, 1986
		13. NUMBER OF PAGES 37
14. MONITORING AGENCY NAME & ADDRESS (if different from Controlling Office) Office of Naval Research 1030 Green Street Pasadena, CA 91106		15. SECURITY CLASS. (of this report) Unclassified
		15a. DECLASSIFICATION/DOWNGRADING SCHEDULE
16. DISTRIBUTION STATEMENT (of this Report) Unlimited		
17. DISTRIBUTION STATEMENT (of the abstract entered in Block 20, if different from Report)		
18. SUPPLEMENTARY NOTES		
19. KEY WORDS (Continue on reverse side if necessary and identify by block number) Free electron laser, two-stage FEL, quasioptical cavity, grazing-incidence mirrors, helical wiggler, dipole ring, electrostatic accelerator, dynamitron		
20. ABSTRACT (Continue on reverse side if necessary and identify by block number) The basic concept and constraints on two-stage free electron lasers are summarized, and the KMS Fusion two-stage FEL design employing a helical wiggler and quasioptical cavity is described. Recent work is reviewed in the areas of cavity design, modeling of the field of a permanent-magnet helical wiggler, fabrication and calibration of permanent magnet dipole rings, and electrostatic accelerator design. A list of publications resulting from this project is given in the references.		

DTIC
SELECTED
AUG 13 1986
S D D

FILE COPY

86 8 13 094

Final Report on Two-stage FEL Research at KMS Fusion, Inc.

Introduction

This is a final report on a project to investigate the feasibility of a two-stage free electron laser (FEL) for the Office of Naval Research. This project was funded at a level that permitted us to investigate concept feasibility, perform some hardware design, develop prototypes of some hardware components, experimentally test cavity design concepts, investigate appropriate accelerator technology, and develop computer simulation codes to model the FEL interaction. No money will, however, be made available to perform a two-stage FEL experiment.

The objective of this report, therefore, will be to document the work that has been performed up to now, so that the knowledge gained will be available if a two-stage FEL employing our proposed design is built in the future. The report also describes technology developed during this program which may be of general applicability in the areas of free electron lasers, magnetic structures and accelerator technology. A number of papers and reports have already been published on this work¹⁻²³ and these will be referenced throughout the report.

In a two-stage FEL a relatively low-energy relativistic electron beam (~ a few MeV) is used to produce long-wavelength radiation (~ 1 mm) in a conventional magnetic wiggler. This long-wavelength radiation builds up to high intensity in a low-loss cavity and acts as an electromagnetic wiggler or pump field for producing short-wavelength radiation (~ 1 μm). The electron beam producing the long-wavelength radiation can be the same beam that produces the short-wavelength light, or separate electron beams could be used to produce the long- and short-wavelength light.

Two-stage free electron lasers have two potential advantages over conventional single-stage FELs. First, a smaller more compact accelerator could be used to drive the FEL, and second, the shielding requirements would be greatly reduced compared with a single-stage short-wavelength FEL. Single-stage FELs require a beam of at least 100 MeV to produce short-wavelength light at the fundamental frequency. At energies above 10 MeV, electrons hitting the wall of the transport system can produce x-rays with sufficient energies to produce (γ, n) reactions in the surrounding material. Over a

<input checked="" type="checkbox"/>
<input type="checkbox"/>
<input type="checkbox"/>
ies
or



A-1

meter of concrete shielding would be required to provide protection for personnel from this radiation. For accelerators with beam energies below 10 MeV, materials can be chosen for which x-ray energies are below threshold for neutron production and only a few mm of lead shielding would provide adequate protection.

Alternatives to the two-stage FEL

Two alternatives to the two-stage FEL have been proposed for reducing the electron beam energy needed to obtain short-wavelength radiation. These are: 1) very short period magnetic wigglers and 2) operation at a higher harmonic of the resonant frequency. These alternative techniques could be useful for reducing the electron energy needed to produce light at a given wavelength by a factor of a few, thereby reducing the overall cost of the accelerator needed to produce the radiation. They would not, however, be as effective as a two-stage FEL in producing reductions of over an order of magnitude in the required electron energy.

The wavelength of radiation produced at resonance in an FEL with a magnetic wiggler is given by

$$\lambda_L = \frac{\lambda_w}{2\gamma^2} (1 + K^2) \quad (1)$$

where, in mks units,

$$K = \frac{e \lambda_w B_w}{2\pi m c} . \quad (2)$$

λ_w is the wiggler periodicity, B_w is the on-axis wiggler field and γ is the ratio of total electron energy to electron rest mass. For a given electron energy λ_L can be reduced by reducing λ_w . Techniques have been developed for producing wigglers with very short periods.²⁴

The major deficiency of very-short-period wigglers is the small aperture needed to obtain useful field strength. Typically the aperture size is the order of or less than the wiggler period. Problems may arise in constraining high-current low-energy beams to pass through the wiggler without hitting the wall of the beam line. Clipping of the optical beam could also be a problem. Some wiggler designs have been proposed in which only one magnetic surface is used, and the electron beam skims along this surface. In addition

to producing both weak and distorted fields, the tolerances for these open-faced wigglers are not significantly lower than for small-aperture wigglers if useful radiation is to be produced.

The problem of small aperture size can be eliminated if a long-wavelength (~ 1 mm) electromagnetic wave is used to interact with the electron beam. Rather than worrying about whether the aperture would be too small, a waveguide may be needed to confine the long-wavelength pump-field radiation to obtain sufficient intensity over a long interaction region. The energy density in the electromagnetic wave must be comparable to the energy density that would be needed in a static magnetic field to produce the same strength interaction. The wavelength of the short-wavelength radiation produced by the second stage of a two-stage FEL is given by

$$\lambda_L \approx \frac{\lambda_p}{4\gamma^2} \quad (3)$$

where λ_p is the wavelength of the long-wavelength pump field. The wavelength of a two-stage FEL employing a single electron beam is given by

$$\lambda_L = \frac{\lambda_w}{8\gamma^4} (1 + K^2) \quad (4)$$

The γ^{-4} dependence of wavelength on energy is the reason why short-wavelength can easily be achieved with low electron energy in a two-stage FEL.

The second alternative to the two-stage FEL is direct production of higher harmonics in a single-stage FEL.²⁵ The gain in the harmonics at a given electron energy is a rapidly decreasing function of harmonic number, and it is not clear that any efficiency enhancement techniques could be used with higher harmonics. Also, the permissible effective energy spread decreases as $\frac{1}{n}$ where n is the harmonic number. Nevertheless, operation at a higher harmonic could be used to reduce the electron energy needed to obtain radiation at a given wavelength, but not by as large a factor as for the two-stage FEL.

Requirements for a two-stage FEL

For the two-stage FEL to compete with continuously operating high-power

conventional lasers and other types of free electron lasers it must satisfy a number of requirements. Some of these are:

1. ability to operate continuously
2. high efficiency
3. high power.

Other desirable qualities are tuneability, good beam quality, and relatively low cost for the power obtained. Other research groups have studied two-stage FELs,^{26,27} but in most cases these studies were directed toward proof of principle experiments. Our studies have concentrated on approaches which, if successful, would scale to relatively high-power high-efficiency continuously operating devices. This approach has resulted in decisions to pursue specific technologies that would be appropriate to meet these objectives.

The characteristic of a two-stage FEL that has the greatest impact on its design is the height of the second-stage phase space bucket. The effective energy spread of the electron beam should not be larger than this bucket height. Electron energy conversion in a constant period wiggler cannot be greater than the bucket height. The full bucket height is given by

$$\begin{aligned} \Delta\gamma_b &= \frac{e\lambda_p}{\pi m c^2} (E_L E_p)^{\frac{1}{2}} && \text{(electromagnetic pump)} \\ &= \frac{e\lambda_w}{\pi m c} \sqrt{\frac{2}{c}} (E_L B_w)^{\frac{1}{2}} && \text{(magnetic pump)} \end{aligned} \quad (5)$$

The bucket height is directly proportional to the pump field period, and, as this period is decreased to produce shorter-wavelength light, the bucket height, permissible beam energy spread, and conversion efficiency must also decrease. This is true both for the second-stage of a two-stage FEL and for short-period magnetic wigglers. For example, for an electron energy of 4 MeV, a pump field intensity of 10^8 w/cm², a second-stage laser intensity of 10^3 w/cm², and a pump field wavelength of 1 mm, the full bucket height would be 3.8×10^{-5} of the electron energy. It appears that effective energy spreads in the few $\times 10^{-4}$ range can be achieved using an electrostatic accelerator as the beam source. This means that, for successful operation of a two-stage FEL, pump field intensities greater than 10^9 w/cm and laser intensities greater than 10^5 w/cm² are probably needed. Lower laser

intensities would, of course, be present during buildup from spontaneous emission, but these higher values should be attained at the operating point for the second stage cavity. Increasing the pump field wavelength somewhat may also be desirable.

There is a penalty for increasing the pump field intensity and pump field wavelength. The penalty is that the energy spread produced in the first stage may become so great that recovery of the electron beam will be difficult. For example, with a long-wavelength intensity of 10^9 w/cm², a magnetic field of 1 kG and a magnet period of 9.08 cm (produces 1-mm radiation at 4 MeV) the full bucket height in the first stage is 46% of the electron energy (equation (5)). If the electrons stay in this field long enough to execute one synchrotron oscillation a comparable energy spread will be produced in the beam.

The two effects of very small second-stage buckets and very large first-stage buckets are major constraints in the design of a two-stage FEL. Because the second stage buckets are small, a very low energy spread, very low emittance beam must be used. The low conversion efficiency indicates that some method of efficiency enhancement is probably needed in the second stage to produce a practical device. The large first-stage buckets indicate that a large energy spread will be produced in the beam exciting the first stage. If recovery of this beam is critical for laser operation, such as when an electrostatic accelerator is used as a driver, the first-stage intensity achievable might be limited by the energy spread the return beam line can accept.

The KMSF two-stage FEL design

We have developed a two-stage FEL design concept that appears to overcome the major obstacles for a practical system. The design includes both the cavity and the accelerator, since the laser must be optimized as a complete system. The cavity design is shown conceptually in Figure 1.

In this design the long wavelength beam is confined in a waveguide to provide a long high-intensity interaction region. The only practical technique for enhancing second stage gain is to accelerate electrons trapped in the second stage buckets with an axial electric field. An axial electric field can only be set up inside a conducting waveguide if the waveguide is segmented. A waveguide made up of a large number of conducting rings can propagate modes that have only azimuthally directed wall currents. This can

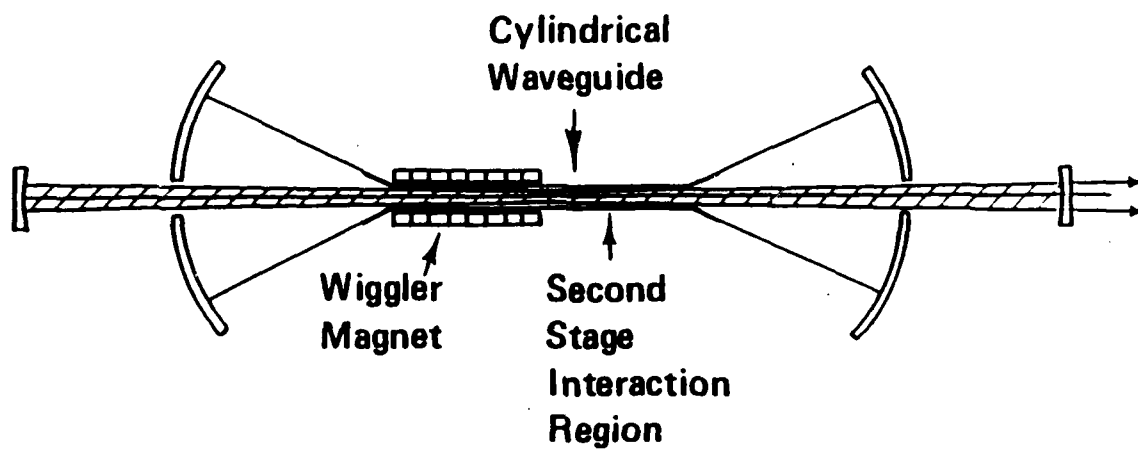


Figure 1. Conceptual design of a two-stage FEL cavity

be achieved in a cylindrical waveguide, for which the lowest loss mode is the TE_{01} annular waveguide mode. We have, therefore, chosen to incorporate a cylindrical waveguide into our cavity design. The mode that would be produced preferentially is the azimuthally polarized TE_{01} waveguide mode, and an annular electron beam would most efficiently excite this mode.

A helical wiggler is needed to uniformly excite the TE_{01} mode. For practical continuous operation a permanent-magnet helical wiggler would be best, especially since very high fields are not needed in the wiggler. A second critical choice of parameters for this system, after the choice of the type of waveguide and mode structure, was the decision to pursue development of a permanent-magnet helical wiggler.

The high intensity long-wavelength radiation must be contained in a low-loss cavity for efficient two-stage FEL operation, since none of the long wavelength radiation is used as output and any loss reduces system efficiency. Long-wavelength radiation intensity is very low on the waveguide walls, but the beam must be expanded to prevent damage to the cavity end mirrors. The cavity design must also permit short-wavelength radiation to be removed without incurring significant long-wavelength radiation losses.

A quasioptical cavity design was chosen to accomplish these objectives. Long-wavelength radiation leaving the waveguide expands by diffraction to the cavity end mirrors and is reflected back into the waveguide. Short-wavelength radiation diffracts less and can be extracted through a hole in the center of the mirrors. A nested two-stage cavity design results. Long-wavelength losses are further minimized because the annular beam has a null on-axis at the location of the holes in the inner mirrors.

The major loss mechanism for this quasioptical cavity is mode conversion at the waveguide-free-space interface. Radiation leaving the waveguide as a single waveguide mode can be converted into a number of free space modes, although most of the radiation will be converted to the TEM_{01}^* annular free space mode. Different modes suffer different phase shifts while transiting the free space region, and the mode pattern created by the radiation returning to the waveguide will not be exactly the same as that for the radiation leaving the waveguide.

We have studied this problem experimentally and theoretically.^{11,23} One solution to the problem is a two-mirror end configuration that produces a 2π phase shift between adjacent free space modes. A second solution would be to use an aspheric end mirror with a surface that matches the shape of the wavefront leaving the waveguide.

A single electron beam is used to operate the FEL with the cavity configuration shown in Figure 1. The electron beam from the accelerator would first pass through the second stage interaction region in which a small quantity of energy would be removed and a small energy spread would be produced in the beam. This energy spread would be negligible compared with the size of the first stage buckets, so the electrons could also be used to excite radiation in the first stage of the FEL.

The basic conceptual design could also be used with two electron beams, one to excite each stage of the radiation. This is shown in Figure 2. A two-beam system offers more flexibility but also more complication. The electron beam used in the second stage develops only a small energy spread, so that energy recovery is no problem. Energy recovery with a large energy spread must still be accomplished with the first-stage beam to permit continuous, efficient system operation. One advantage of having two waveguide segments is that a smaller-diameter waveguide could be used in the second stage to increase pump field intensity while a larger-diameter waveguide could be used in the first stage to decrease long-wavelength radiation intensity and reduce energy spread. Reducing the diameter of the waveguide increases long-wavelength waveguide losses. The diameter of the waveguide for the single-electron-beam design of Figure 1 was chosen to minimize long-wavelength losses while still maintaining a high field intensity in the waveguide. For 1-mm radiation, a 2.4-cm diameter waveguide is needed to keep absorption losses on the order of 0.1% over a distance of a few meters.

The accelerator is an integral part of the two-stage FEL and must be designed to optimize system performance. An electrostatic accelerator with energy recovery appears to be the best accelerator for continuous operation of this type of FEL. Recovery of the electron beam leaving the first stage is the major design problem. The low charging current of conventional electrostatic accelerators also limits the beam current that can be supplied.

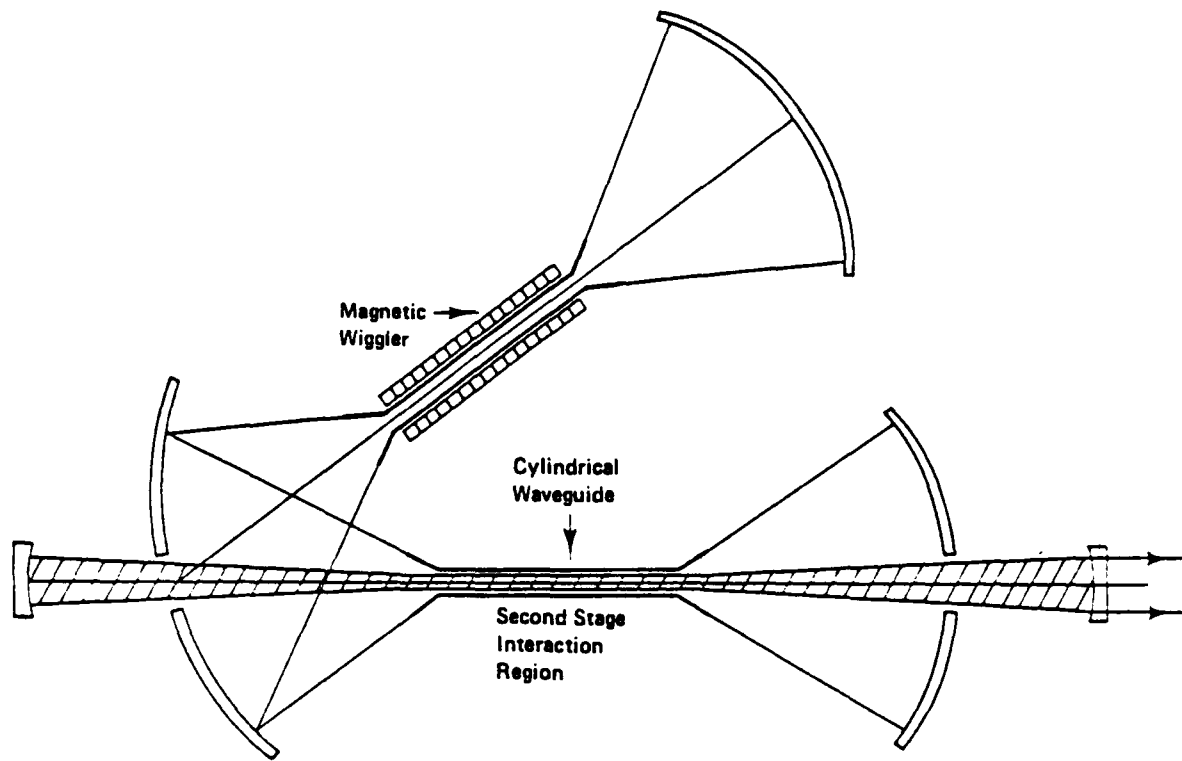


Figure 2. Two-stage FEL cavity in which a separate electron beam could be used for each stage of the interaction.

A conceptual design of an electrostatic accelerator that could provide both high charging current and recover a beam with a large energy spread is shown in Figure 3. Charging current is supplied by an array of stacked power supplies driven by an array of permanent magnet generators. An insulated drive shaft from an electric motor provides power to the generators. An average charging current on the order of 1 amp, which is three orders of magnitude higher than for conventional electrostatic accelerators, could be generated in this way.

The stacked power supplies also serve a second purpose. Current collected on any plate in the return beam line could be returned to the dome of the accelerator through the power supply connected to that plate. This would permit collection of a beam with any energy spread that could be transported back to the accelerator. To increase the size of the energy spread that could be collected, the accelerator should be aligned in the plane of the beam line with the return column of the accelerator located as close as practical to the end of the wiggler.

Propagation of an annular electron beam through the system is more difficult than for a narrow cylindrical beam. The beam does not have to remain annular everywhere in the beam line, but should be annular in the interaction region. Our calculations indicate that a properly injected annular beam will remain annular throughout the wiggler.²¹

In most FEL systems the electrons are focused down into a narrow on-axis beam to increase the current density. In a two-stage FEL with a low energy beam, space charge forces may degrade the emittance if the current density is too high. Space charge forces and effective energy spread due to emittance are minimized in an annular beam. With good energy recovery in the accelerator and a high charging current, currents of hundreds of amps to a kiloamp could probably be achieved in an annular beam, providing enough gain to operate a high-power efficient system.

Recent research results

Over the last year we have investigated a number of key issues impacting the feasibility of the system we have described above.

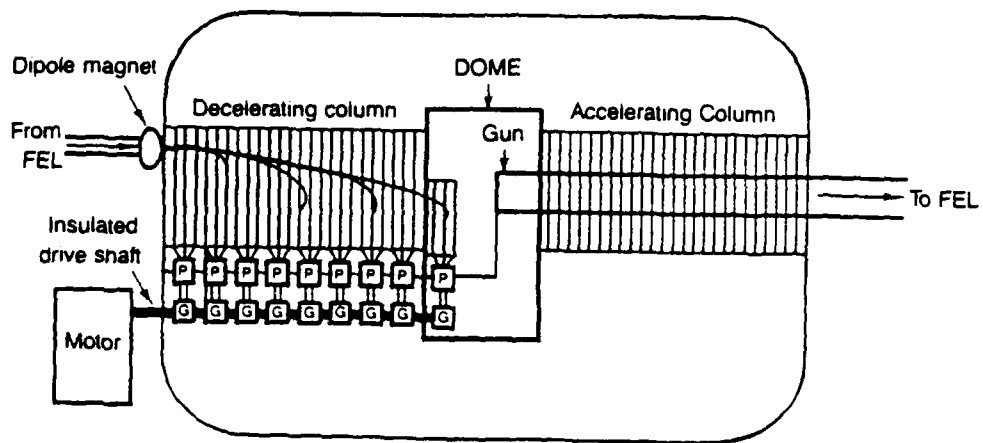


Figure 3. Conceptual design of an electrostatic accelerator that could provide both high charging current and recovery of a beam with a large energy spread.

Work was performed in the following areas:

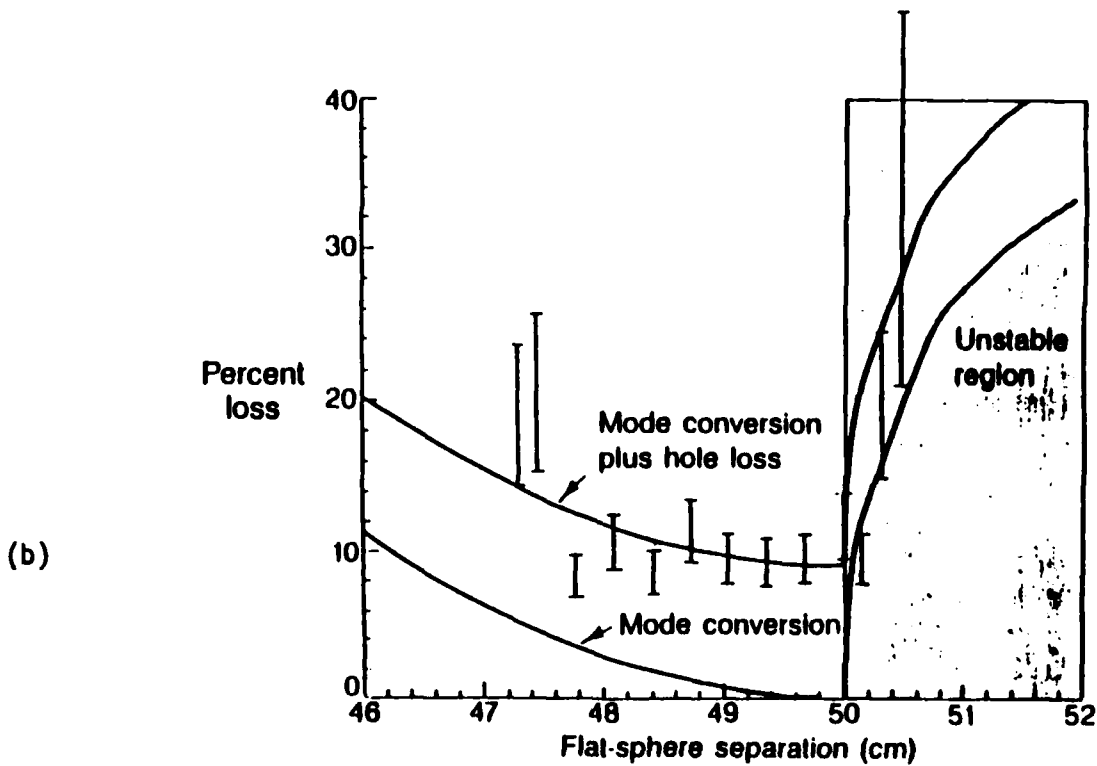
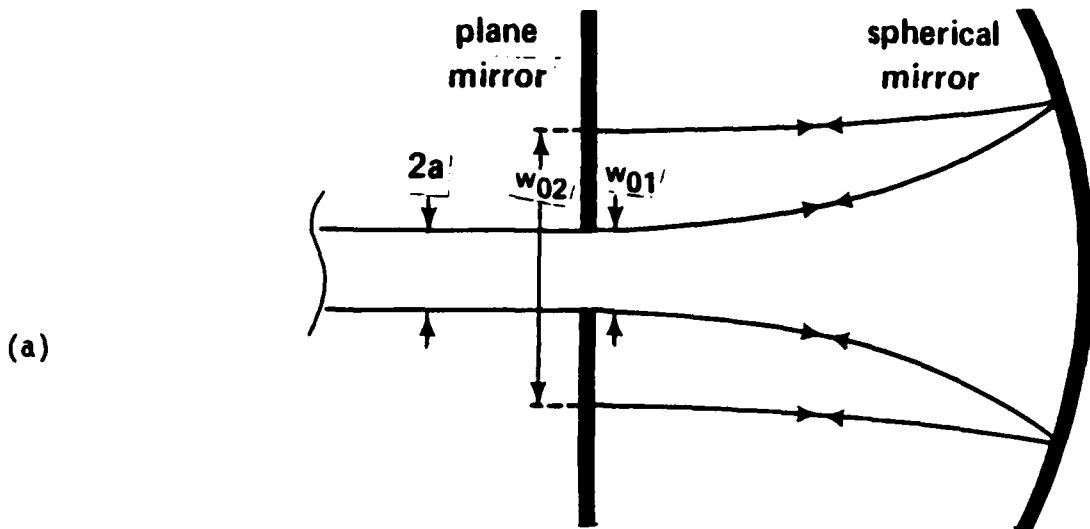
1. Experimental demonstration of the two-mirror end configuration for a quasioptical cavity and comparison with a single-spherical-mirror end configuration.
2. Design of the second stage cavity.
3. Three-dimensional modeling of the field of a permanent-magnet helical wiggler.
4. Fabrication and calibration of dipole rings for a helical wiggler.
5. Development of techniques to calculate the bandwidth of an annular laser beam.
6. Design of a practical high-current electrostatic accelerator.

Long-wavelength cavity experiment

A detailed discussion of the long-wavelength quasioptical cavity experiment is given in reference²². In this experiment, cavity end configurations were tested using a conventional 94 GHz microwave source and mode conversion losses were measured for each case. The two cases were a simple spherical end mirror and a two-mirror end configuration composed of one spherical and one flat mirror. The flat mirror was located at the end of the waveguide (see Figure 4a). Theoretically, mode conversion losses go to zero in the two-mirror configuration as the diameter of the waveguide becomes small relative to the size of the beam on the flat mirror. In our experiment the hole size was larger and the beam diameter on the flat mirror smaller than would be expected in an actual FEL experiment. As a result losses in the TE_{01} mode due to the waveguide hole appear to have dominated losses that could be attributed to different relative phase shifts in adjacent modes. The results are consistent with theory when hole losses are considered, but did not reduce total losses compared to a single spherical end mirror. Funding was not available to perform followup experiments with different ratios of hole size to expanded-beam diameter.

Second-stage cavity design

The second-stage radiation, like the first-stage radiation that produced it, would be in an annular azimuthally-polarized mode. Because of the short



Figures 4. (a) Two-mirror end configuration for reduction of mode conversion losses. (b) Comparison of experimental measurements for losses at waveguide-free-space interface with the theoretical model for mode conversion losses and mode conversion plus hole losses.

wavelength of the second-stage ($\sim 3.2 \mu\text{m}$ for a 4-MeV electron beam and 1-mm-wavelength pump field), mode control would be very difficult in a two-mirror cavity. Very flat mirrors would be needed for the relatively large diameter annular beam.

A four-mirror cavity employing two grazing incidence paraboloid mirrors was investigated for the short-wavelength radiation. This work was reported in reference²³. A schematic of the cavity design is shown in Figure 5. Because of the azimuthal polarization, absorption is minimal on the surfaces of the grazing incidence mirrors.

This four-mirror cavity is very compact compared with other high-power FEL cavity designs employing grazing incidence mirrors. This can be an advantage if one does not wish to have a very long cavity and still avoid damage to the cavity end mirrors. If a very long cavity is acceptable, mirror loading could be less for free electron lasers with narrow on-axis beams than for an FEL with a larger-diameter annular beam. This is because diffraction is greater in a narrow-diameter beam. If one goes out far enough, the loading from a narrow-diameter beam can always be made lower than the loading from a larger-diameter annular beam.

Three-dimensional magnet model

A code has been developed to model the three-dimensional fields of all-permanent-magnet structures. This code calculates the field of a permanent magnet assuming the field can be modeled by a sheet of magnetic charges on the surface of the magnet. The three-dimensional field of a magnetic structure can be calculated by superimposing the fields of the individual magnet pieces. This technique neglects the small demagnetizing effects of the pieces on each other.

This code has been applied to modeling a permanent-magnet helical wiggler. The fields obtained from this model were used in our three-dimensional FEL simulation code to follow trajectories of electrons through the wiggler and fringe fields. This work is described in reference [21]. We found that an annular beam with all the electrons in off-axis rosette orbits retains its shape throughout the wiggler and through the fringe field. This indicates that it should be possible to inject an annular electron beam into the wiggler with the desired orbits with properly designed electron optical components.

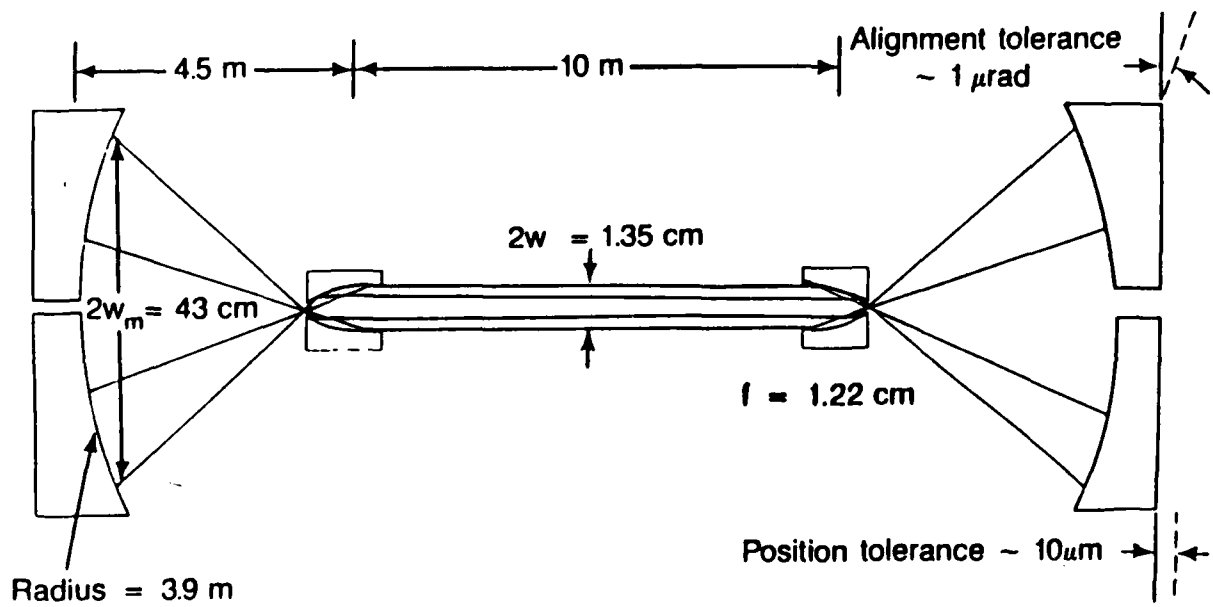


Figure 5. Conceptual design of the second-stage cavity for a two-stage FEL.

To design the electron injection optics, it is necessary to perform a calculation in which the electrons start off with the desired orbits inside the wiggler and then run backward in time through the entrance of the wiggler and the fringe field. This gives the distribution the electrons must have upon entering the wiggler to produce the desired orbits. Assuming the electrons are initially moving on trajectories parallel to the axis of the wiggler, it appears possible to design optical elements that would produce the desired injection condition. We did not have time to modify the code and design the electron optics during this contract period.

Magnet Laboratory

A magnet assembly and calibration facility was set up over the last year, and permanent-magnet dipole rings were fabricated and calibrated. These dipole rings are the building blocks for a permanent-magnet helical wiggler.

Each dipole ring was made up of eight circular arc segments. The segments were mounted in a holding fixture shown schematically in Figure 6. Each arc segment was glued to a brass mount that was held in place by a screw and mounting pins. Segments could be moved radially to tune the field in order to reduce field errors in the interior volume of the dipole ring. Dipole rings were fabricated from both samarium-cobalt and neodymium-iron boron.

The fields of both the individual magnet pieces and the assembled dipole rings were mapped in our laboratory. Individual pieces were mapped by mounting them on a rotation stage and measuring the field components with a Hall probe. The Hall probe was held at a constant position and readings were taken as the piece was rotated. The completed rings were also mounted on a rotational stage and the field was mapped using a three-axis Hall probe mounted on an xyz positioning stage. The Hall probes were calibrated using a nuclear magnetic resonance system and a large dipole electromagnet.

Figures 7 through 9 show data obtained for the main component of the dipole field, B_x , as a function of x , y and z along axes running through the center of the dipole ring. The solid line is the calculated value for this field component obtained using the three-dimensional magnetic-charge-sheet-equivalent code. In the code a remanent magnetic field of 8.5 kG in the

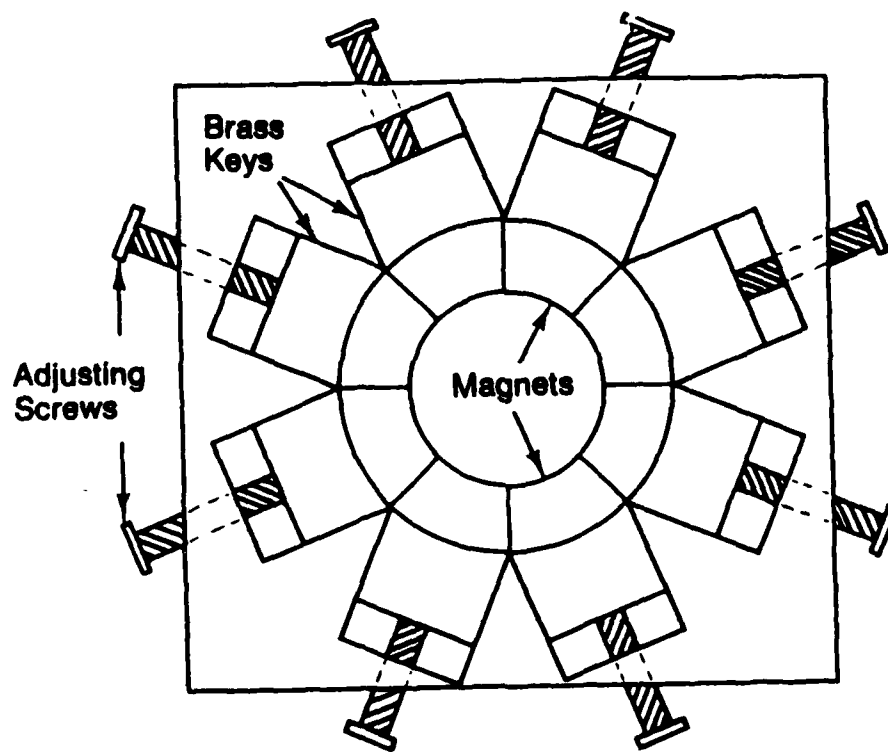


Figure 6. Holding fixture for permanent magnet dipole ring
Each magnet was glued to a brass key. The keys could
be moved radially to tune the field inside the ring.

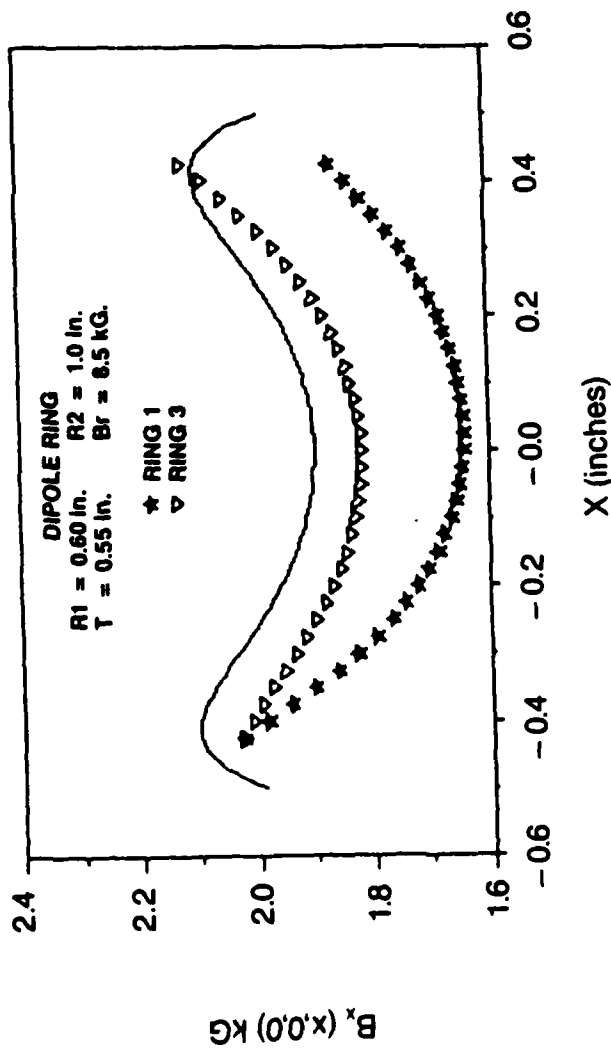
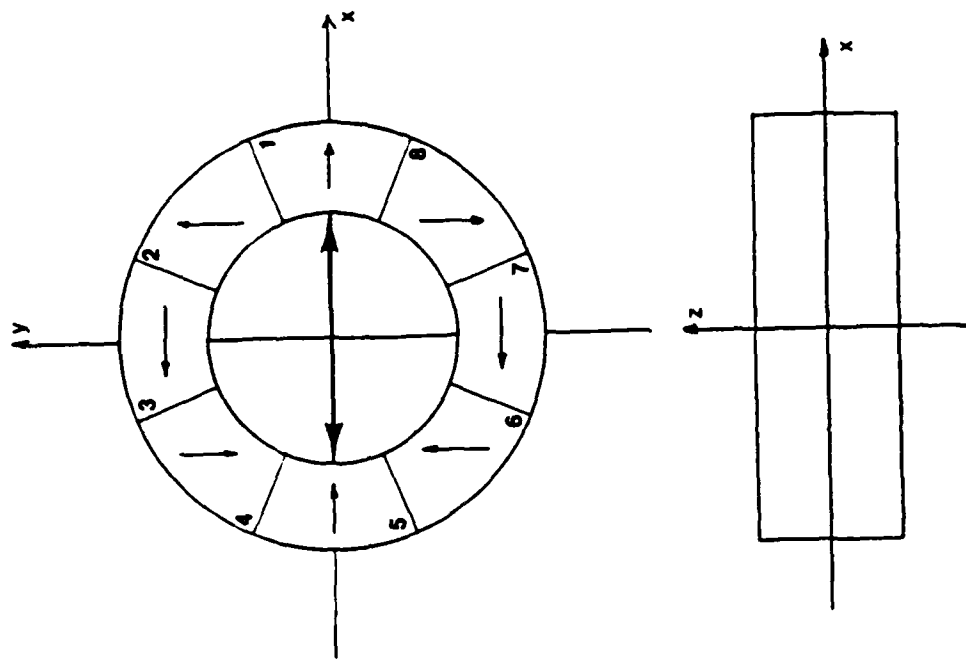


Figure 7. Comparison of experimental and theoretical values of the dominant field component, B_x , of a dipole ring in a scan along the x axis. Two different dipole rings were measured. $R1$ and $R2$ are the radii of the circular arc-segment magnets. T is the thickness of the magnets and B_r is the remanent magnetic field assumed in the calculation.

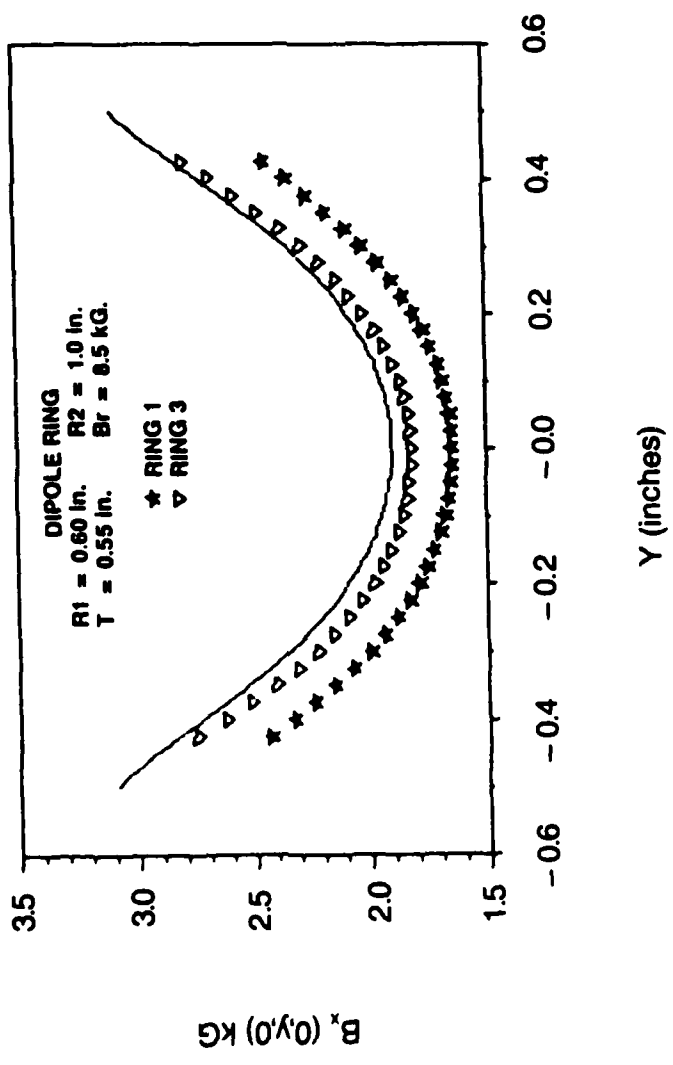
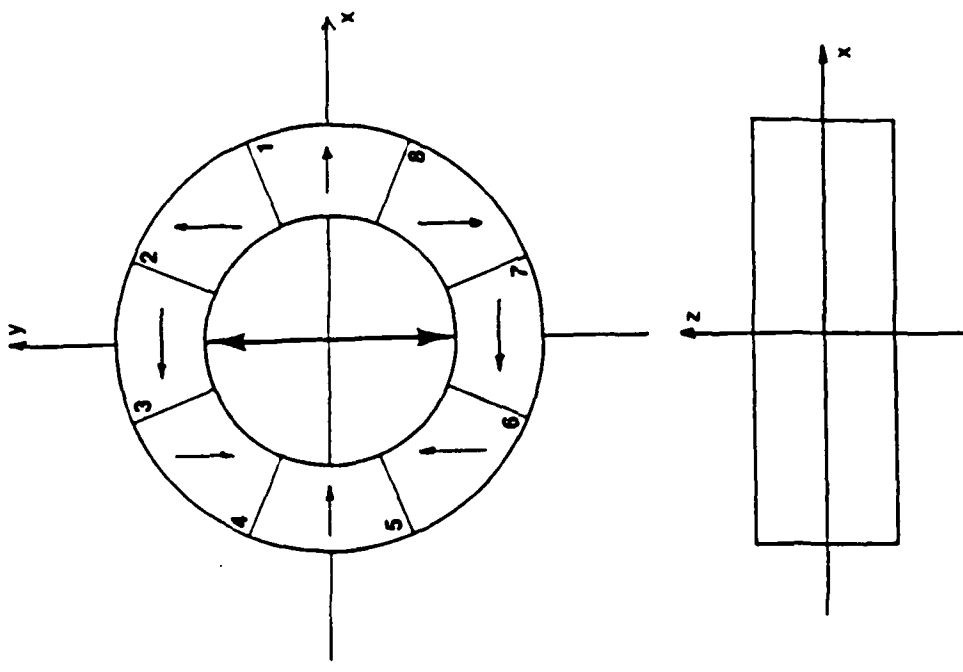


Figure 8. Comparison of experimental and theoretical values of B_x for a scan in the Y direction.

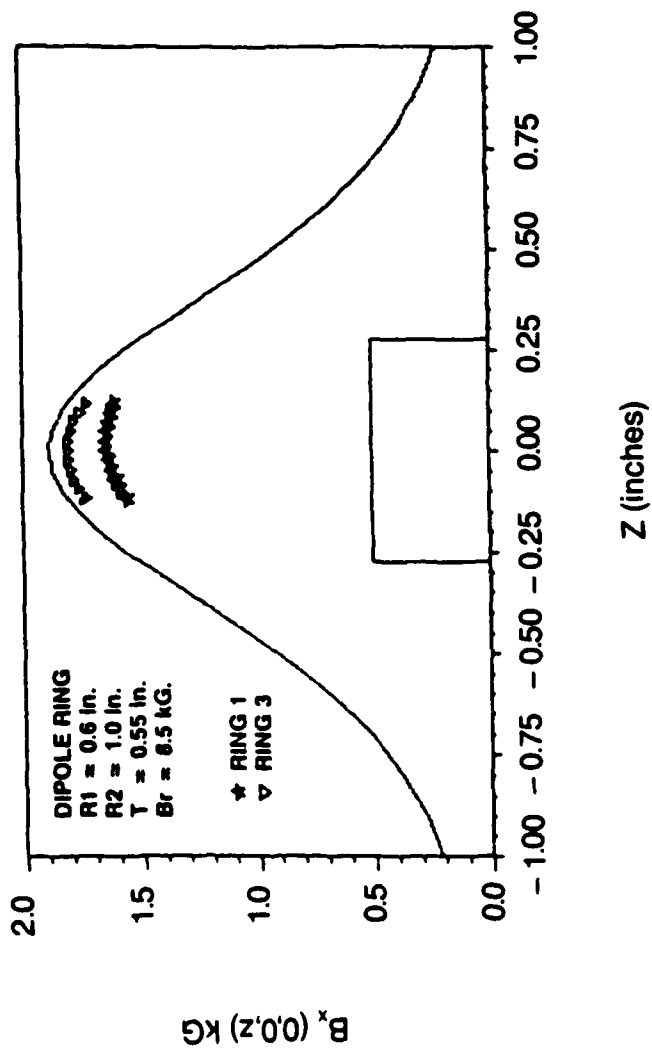
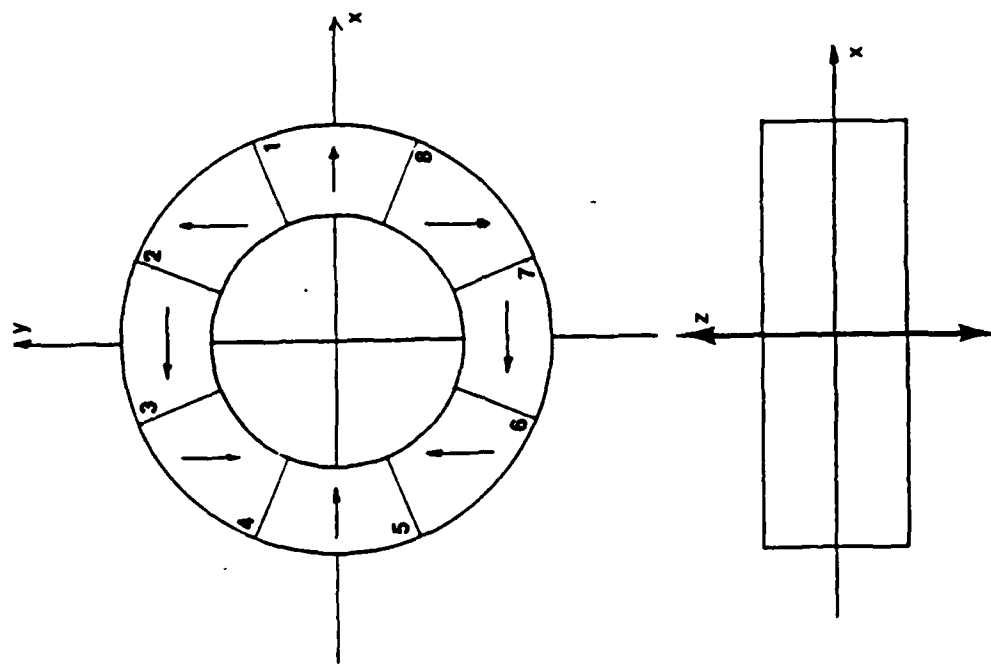


Figure 9. Comparison of experimental and theoretical values of B_x for a scan in the Z direction. The experimental data is limited because of the limited motion of the manipulator stage in the Z direction.

material was assumed with no air gaps between the magnets. The shape of all eight pieces of the ring was assumed to be identical.

Measured field values were always somewhat lower than calculated values, although the shape of the theoretical and experimental curves matched quite well. Differences in the shape of the curves could be unambiguously correlated to variations in the shape of the pieces. For example, in ring 1 piece number 1 was smaller than piece number 5 leading to an asymmetry in the values of B_x along the x axis in Figure 7.

Some of the difference between the magnitudes of the theoretical and experimental curves can be attributed to neglect of demagnetization in the model, which is expected to be a few percent effect. The rest of the difference can be attributed to differences in the remanent magnetic field from ring to ring. This is seen in the difference in field strength between rings 1 and 3. The remanent field for all the pieces of a given ring should be about the same, since all pieces for a single ring were cut from the same block of magnet material.

It should be noted that the field predicted for the inside volume of the dipole ring using our three-dimensional code is quite different than the uniform fields obtained from a two-dimensional calculation, which assumes the dipole ring has an infinite axial extent. The field has a minimum on axis in the central transverse plane due to the finite thickness of the magnets.

The reason for building these rings was to gain experience and identify problems involved in fabricating these types of structures. These rings were the first to be built with circular arc segments rather than trapezoidal-shaped magnets. This geometry was chosen because circular arc segments produce fewer unwanted harmonics than trapezoidal segments. The main problem we encountered in building the rings was obtaining magnets of uniform shape and magnetization. These problems should be overcome with more experience and tighter magnet specifications. An insufficient number of rings were produced during this contract to assemble a helical wiggler.

FEL Theory

A major area of concern for successful two-stage FEL operation is the bandwidth of the radiation produced by the first stage. If the bandwidth is too broad it may reduce gain in the second stage. Broadening of the bandwidth

in a helical wiggler with an off-axis electron beam results because each electron samples a range of magnetic field values, and the beam as a whole occupies a region with significant variation of the magnetic field as a function of radius.

The most direct approach to calculating the bandwidth would be to run the FEL simulation code with a number of closely spaced frequency components. These components could all initially be set to a very low amplitude, and each frequency component would be amplified at each time step by the electron beam. The change in electron energy per time step would be the sum of the losses and gains from each frequency component and the resultant field would be the vector sum of the different field components taking both amplitude and phase into consideration.

Previous computer simulations at KMSF have all been carried out at a single frequency. This frequency was determined by the FEL resonance condition (equation 1). Fine tuning of the frequency was accomplished by calculating the gain for a number of closely spaced single frequencies and choosing the one with the highest gain as the central laser frequency. The code follows a representative sample of electrons one ponderomotive wavelength long in the axial direction with periodic boundary conditions.

This code cannot be used to calculate the gain in a laser beam with several closely-spaced frequencies without modification. The reason is that the length of the ponderomotive bucket is different for each frequency component. Axial beam segments that satisfy the boundary conditions exactly for one frequency component will be unbalanced and produce errors in the calculation of gain at other frequencies. Since the energy transferred to the laser beam is the sum of both positive and negative contributions, and the net transfer may be only a small fraction of the sum of the absolute values of the contributions from each electron, small amounts of uncompensated charge can cause large errors in the result.

We have developed a frequency independent technique to calculate the bandwidth of the laser radiation at saturation. This technique can be used when the beam is azimuthally polarized. When this is the case, all values of the phase

$$\psi = \cos^{-1} \left(\frac{\vec{\beta}_L \cdot \vec{E}_L}{|\beta_L| |E_L|} \right)$$

in a helical wiggler with an off-axis electron beam results because each electron samples a range of magnetic field values, and the beam as a whole occupies a region with significant variation of the magnetic field as a function of radius.

The most direct approach to calculating the bandwidth would be to run the FEL simulation code with a number of closely spaced frequency components. These components could all initially be set to a very low amplitude, and each frequency component would be amplified at each time step by the electron beam. The change in electron energy per time step would be the sum of the losses and gains from each frequency component and the resultant field would be the vector sum of the different field components taking both amplitude and phase into consideration.

Previous computer simulations at KMSF have all been carried out at a single frequency. This frequency was determined by the FEL resonance condition (equation 1). Fine tuning of the frequency was accomplished by calculating the gain for a number of closely spaced single frequencies and choosing the one with the highest gain as the central laser frequency. The code follows a representative sample of electrons one ponderomotive wavelength long in the axial direction with periodic boundary condition.

This code cannot be used to calculate the gain in a laser beam with several closely-spaced frequencies without modification. The reason is that the length of the ponderomotive bucket is different for each frequency component. Axial beam segments that satisfy the boundary conditions exactly for one frequency component will be unbalanced and produce errors in the calculation of gain at other frequencies. Since the energy transferred to the laser beam is the sum of both positive and negative contributions, and the net transfer may be only a small fraction of the sum of the absolute values of the contributions from each electron, small amounts of uncompensated charge can cause large errors in the result.

We have developed a frequency independent technique to calculate the bandwidth of the laser radiation at saturation. This technique can be used when the beam is azimuthally polarized. When this is the case, all values of the phase

$$\psi = \cos^{-1} \left(\frac{\hat{B}_\perp \cdot \hat{E}_L}{|B_\perp| |E_L|} \right)$$

are represented in a cross sectional sample of the beam (see Figure 10). Therefore, instead of following an axial segment of the electron beam one ponderomotive wavelength long through the wiggler, we can simulate the propagation of a cross sectional distribution in which the electrons initially occupy a uniform distribution of phases in phase space. This cross sectional distribution represents all phases in the ponderomotive bucket independent of frequency, so that a number of frequencies can be run simultaneously and the interaction of the various frequency components through the electron distribution can be calculated.

Simulation runs using a cross sectional distribution do not, however, correctly predict the gain profile of the beam along the wiggler. This is because the cross sectional distribution we simulate in the wiggler is not axisymmetric, and all electrons are not at the same radial position simultaneously. The distribution we chose to follow is the locus of all electrons with axisymmetric orbits having the same radial excursion in the wiggler. The locus of these points at a given axial location is not axisymmetric.²¹ Therefore, although all phases are represented in the distribution, the bucket height for different electrons may be different. The net result is that the saturation intensity and laser bandwidth at saturation are correctly predicted, but the gain profile along the wiggler leading up to saturation is incorrect.

Although this technique has its limitations, it still can be used to provide information on bandwidth. We have used this method to investigate the shift in central wavelength produced by the interaction of the various components of a multifrequency beam with the electron distribution. Since radiation emitted at shorter wavelengths can be absorbed by electrons instantaneously at resonance with a longer wavelength, there is a net shift of the central frequency in the long-wavelength direction.

This wavelength shift is shown in Figure 11. The figure shows gain as a function of laser wavelength on a single pass through the wiggler for a number of different laser wavelengths. In the uncoupled case a number of separate single-frequency gain calculations were performed. Input intensities at all frequencies were identical. In the coupled case, gain was calculated for all frequencies simultaneously.

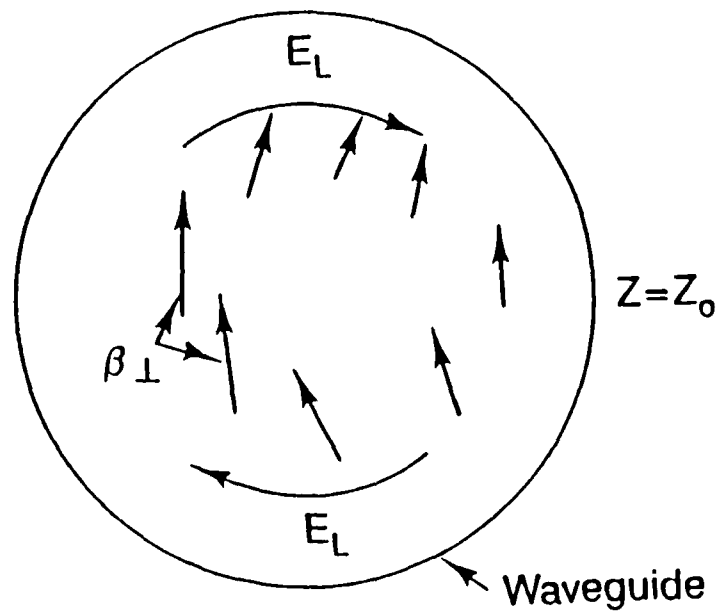


Figure 10. All values of the phase angle between $\hat{\beta}_\perp$ and \vec{E}_L are represented in a cross sectional sample of an annular electron beam and a laser beam with azimuthal polarization.

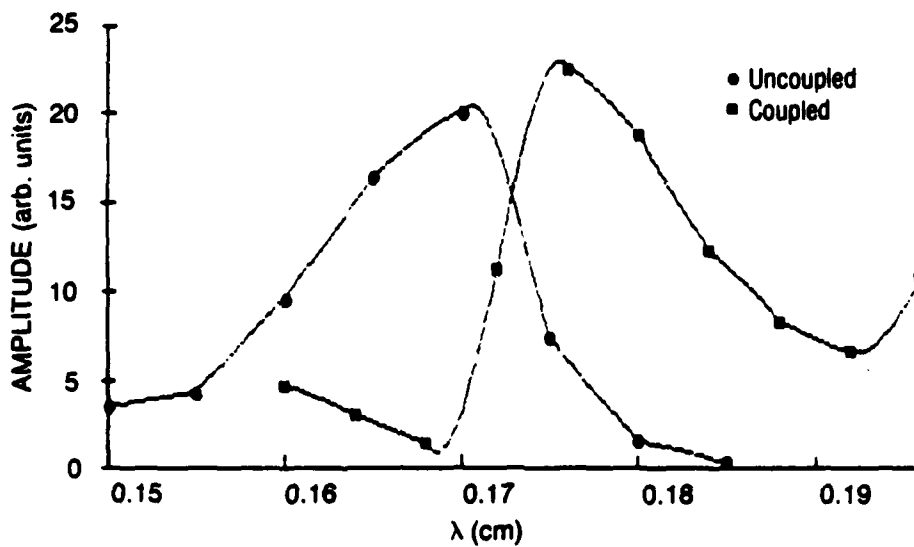


Figure 11. Laser gain in the TE_{01} mode as a function of wavelength on a single pass through the wiggler calculated one wavelength at a time (uncoupled) and for a band of wavelengths simultaneously (coupled) using a cross sectional electron distribution.

The graph of Figure 11 does not indicate the bandwidth that would be produced in the laser under normal operating conditions. It is simply the gain resulting from a single pass through the wiggler with constant input intensities for all components. The bandwidth observed during laser operation would be the result of multiple passes in the optical cavity and should be considerably narrower.

The calculations performed to obtain the data shown in Figure 11 were for a thin filament of electrons, all in orbits with identical excursions about a constant mean radius. A more realistic calculation would include a number of such filaments as well as a number of different laser frequencies. During this contract period we succeeded in developing a technique for investigating bandwidth, but did not have the time to apply this technique to a large number of more realistic calculations.

Accelerator design

Electrostatic accelerators appear to be the accelerators of choice for a low-voltage two-stage FEL. The reason is that they can produce a very high quality beam and high current when there is current recovery. Overall efficiency is also high. The deficiencies of the electrostatic accelerator are very low charging current, which limits either the current or the pulse length, and the small energy loss and energy spread that can be tolerated for energy recovery.

A conceptual design for an accelerator that could overcome these problems was described earlier in this report, but development of the accelerator would be a major project in itself. We have therefore tried to determine whether any existing accelerator design could be modified to achieve the same results.

The electrostatic accelerator design that comes closest to meeting the needs of this experiment is one that has a parallel-coupled voltage multiplier charging circuit. This type of accelerator is also referred to as a dynamitron.²⁸ Accelerators of this type have already been built in relatively large numbers and have been in use for over 20 years in industrial processing. A modified version of this accelerator may be appropriate for the two-stage FEL application.

The basic design of the charging circuit of the dynamitron is shown in Figure 12. The high-voltage terminal is charged by means of a series of

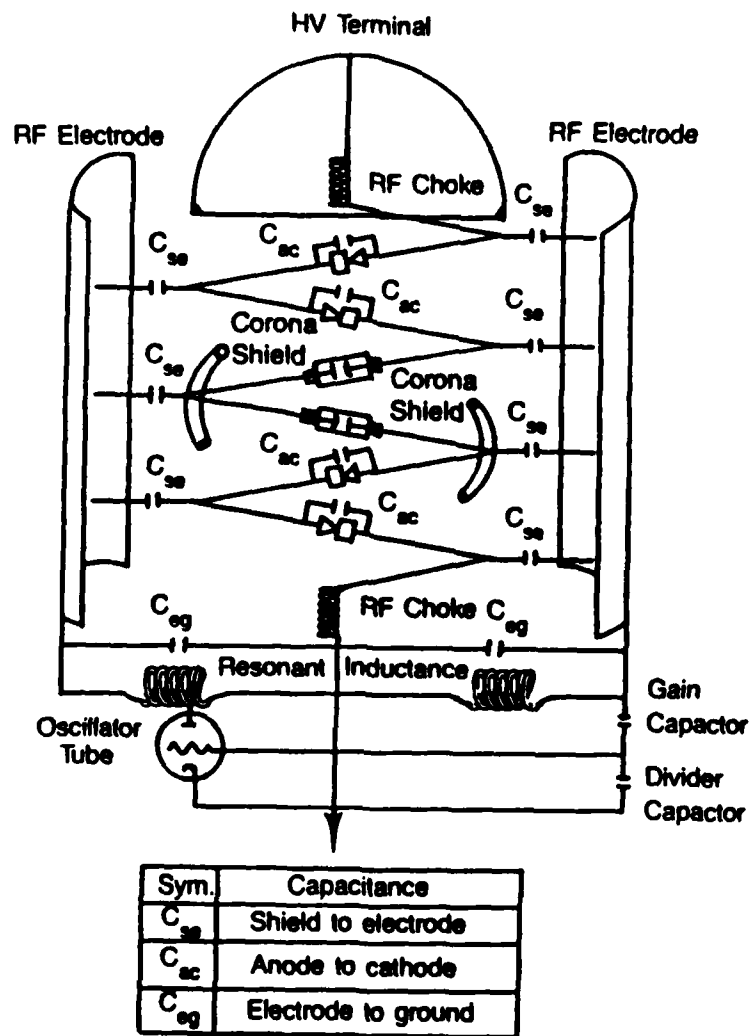


Figure 12. Schematic of the charging circuit of a dynamitron accelerator.

rectifiers that permit charge to flow up a column of corona rings. In a standard dynamitron a stack of semicircular corona half-rings are located between two large conducting plates. The two plates act as a large capacitor. When a voltage is applied to the plates, an induced charge builds up on the half-rings between the plates. When the field is reversed, the charge accumulated on one corona half-ring is transferred to an opposite half-ring at the next highest voltage increment through a rectifier, or diode array, connecting the two half-rings. By providing an oscillating voltage on the outer plates, charge is continually transported from ground to the high-voltage terminal.

The amount of charge accumulated by a half-ring is a function of the magnitude of the oscillating voltage and the capacitance C_{se} between a half-ring and its nearest RF electrode. If ΔV is the amplitude of the voltage on an RF electrode plate relative to ground, N is the number of corona half-rings, and I is the current that must be supplied to make up for losses, the voltage, V , that can be produced on the high-voltage terminal is²⁹

$$V = \left(\frac{N}{k}\right) \left(\Delta V - \frac{I}{fC_{se}}\right) \quad (1)$$

where

$$k = 1 + 4 \frac{C_{ac}}{C_{se}} \quad (2)$$

C_{ac} is the shunt capacitance between corona rings and k is a coupling coefficient. k is the factor by which the voltage gain is reduced as a result of the shunt capacitance. In a standard dynamitron C_{ac} is comparable to C_{se} so that $k \approx 5$. The peak-to-peak voltage between the two RF electrodes is $2 \Delta V$.

For a typical commercial dynamitron $\Delta V = 150$ kV, $N = 80$ and $f = 120$ kHz. Using $C_{se} = 4$ pf and $k = 5$, a voltage of 1 MV could be maintained with a continuous current loss of 40 amp. With no losses, the voltage for this example would increase to 2.4 MV. These values are inadequate for our application, but fairly straightforward upgrades of this type of accelerator, which do not exceed state of the art technology, could raise the performance of the accelerator to a level of interest for a high-power two-stage FEL.

There are a number of areas where improvements in performance could be obtained. Each one would provide an incremental increase in voltage or

current. When taken together these improvements could result in an accelerator with a voltage of about 10 MV and a charging current of up to 1 amp. Including energy recovery could result in an average continuous current on the order of tens of amperes. Since energy could be collected along the decelerating column as well as in the dome, energy extraction of at least 10 percent of the electron beam energy into the short-and long-wavelength electromagnetic beams would be possible.

Some simple steps that could be taken to improve the performance of the dynamitron would be:

1. Increase the number of stages N
2. Use a higher frequency oscillator to increase f
3. Increase the voltage on the RF electrodes to increase ΔV
4. Increase the size of the device to increase C_{se} .

The number of stages in the dynamitron could easily be increased to about 200. Higher voltage and higher frequency components could also be used. Commercially available oscillators could operate at a frequency of about 500 kHz. The voltage on the RF electrode is produced using step-up coils located at the base of the charging column. The primary limit on the electrode voltage is breakdown in the coils. Larger coils could be designed to operate at voltages up to 400 kV. The voltage is produced by an array of coils operating in parallel so that increasing the size of the coils would not prevent operation at a few times higher frequency. A scaling of the device to increase capacitance by a factor of about two is also not unreasonable.

Figure 13 shows a graph of voltage as a function of loss current for an upgraded dynamitron with $N = 200$, $V = 400$ kV, $f = 500$ kHz and $C_{se} = 8$ pf. Peak voltage with no losses is 16 MV. With an average loss of 1 amp the continuous voltage would be 6 MV. The same input power would be required to maintain 6 MV on the dome with an average loss of 10% of the energy of a 10-amp beam as with a loss of 100% of the energy in a 1-amp beam.

The voltage or charging current could be increased even more by optimally utilizing the RF electrode voltage. Each corona half-ring utilizes only one-half of the RF cycle to transmit current. Fully utilizing the RF cycle could result in a doubling of the charging current or a doubling of the accelerator voltage for a given current loss.

The two large opposing electrodes that supply the charging electric field produce a field that is oscillating in magnitude but constant in direction. If a field were produced that were constant in magnitude but rotated around

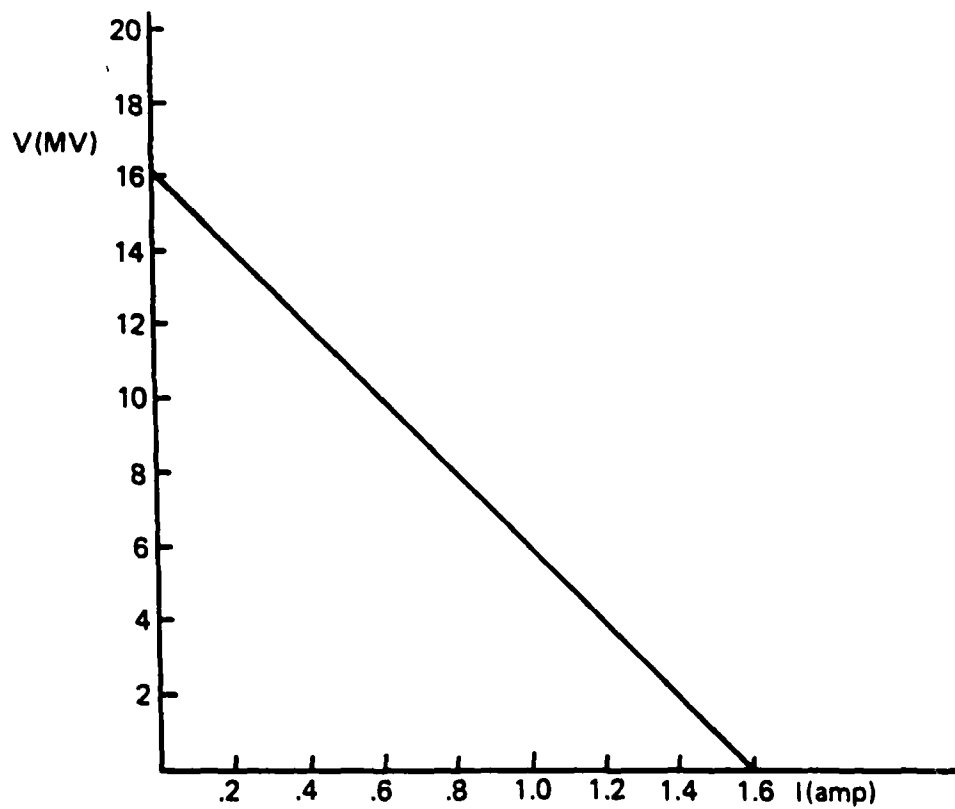


Figure 13. Voltage as a function of equivalent current loss for a dynamitron with $N = 200$, $k = 5$, $\Delta V = 400$ kV, $f = 5 \times 10^5$ sec^{-1} and $C_{se} = 8$ pf. A single pair of electrodes is assumed.

the axis of the accelerator, it would also charge the corona stack, but could do this with the corona ring segments oriented in any direction relative to the field. A rotating field could be achieved by dividing the oscillator driving coil into three coils driven at different phases connected to three pairs of electrode plates positioned around the circumference of the device.

Three stacks of corona ring segments could be used to charge the terminal. These stacks could be more efficiently designed than existing corona ring segments, because the voltage gaps at the ends of the segments would have lower fields due to the polyphase configuration. Even though smaller segments would be used, the charging capacitance would not be reduced proportionately, because the smaller gaps would increase the total capacitance.

A major advantage of this configuration is that it reduces the coupling factor k in equation (2) from a value of 5 to a value of about 2. This means that each stage of the charging cycle would work more efficiently, and fewer steps would be needed to achieve the desired terminal voltage.

Our conclusion from these studies is that a modified dynamitron-type accelerator could supply the current and power needed for a high-power two-stage FEL (> 1 kW average output power in the second stage). It has the advantage over an accelerator incorporating an array of stacked power supplies that no rotating machinery is needed and that the development would consist of upgrading existing designs rather than developing an entirely new type of accelerator.

Conclusions

Our overall conclusion is that a two-stage FEL could be both feasible and practical. There are still a number of issues that need to be resolved, but we have found no problems that would prevent the two-stage FEL from operating at all. The two-stage FEL would always be less efficient than a single-stage device because all of the energy put into the first stage is essentially lost. Output power would probably be less than from a single-stage high-power short-wavelength FEL, but the accelerator would be much smaller and less expensive and personnel shielding requirements would be minimal.

References

1. H. R. Hiddleston and S. B. Segall, "Equations of motion for a free electron laser with an electromagnetic pump field and an axial electrostatic field," IEEE J Quantum Electron QE-17, 1488 (1981)
2. H. R. Hiddleston, S. B. Segall and G. C. Catella, "Variable period free electron laser amplifier simulation studies," in Physics of Quantum Electronics, Volume 7, page 729, S. F. Jacobs, H. S. Pilloff, M. Sargent, M.O. Scully and R. Spitzer, eds., Addison Wesley (1980)
3. W. B. Colson and S. B. Segall, "Energy transfer in constant period free electron lasers," Appl. Phys. 22, 219 (1980)
4. H. R. Hiddleston, S. B. Segall and G. C. Catella, "Gain-enhanced free-electron laser with an electromagnetic pump field," in Physics of Quantum Electronics, Vol 9, page 849, S. F. Jacobs, G. T. Moore, H. S. Pilloff, M. Sargent, M. O. Scully and R. Spitzer, eds., Addison Wesley (1982)
5. S. B. Segall, H. R. Hiddleston and G. C. Catella, "The application of free electron lasers to the transmission of energy in space," ibid Volume 9, page 1013 (1982)
6. T. Speziale and W. B. Colson, "Axial expansion of the electron pulse in a free electron laser," ibid Vol. 8, page 489 (1982)
7. S. B. Segall, "Resonator cavity design for a two-stage FEL experiment," Journal de Physique Vol 44, 383 (1983)
8. S. B. Segall, H. R. Hiddleston, H. Takeda, S. Von Laven, R. Holsinger, J. Ward, R. Richardson and W. B. Colson, "Review of Two-stage FEL Research at KMS Fusion (January through September 1982)," DTIC Report AD-A128623, KMSF Report number KMSF-U1307, January 21, 1983.

9. H. Takeda and S. B. Segall, "Amplifier optimization study for an FEL wiggler with a helical magnetic field and an axial electric field," IEEE Trans Nucl Sci NS-30, 3112 (1983)
10. S. B. Segall, H. Takeda, S. Von Laven, P. Diament and J. F. Ward, "The KMS Fusion, Inc. two-stage free-electron laser program," in Free Electron Generators of Coherent Radiation, C. A. Brau, S. F. Jacobs, M. O. Scully, eds., Proc SPIE 453, 177 (1984)
11. S. Von Laven, S. B. Segall and J. F. Ward, "A low loss: quasioptical cavity for a two-stage free electron laser," *ibid* p. 244 (1984)
12. S. B. Segall, "Annual Summary Report for 1 October 1983 through 30 September 1984," DTIC Report AD A 148 951, KMSF Report number KMSF-U1526, Oct. 24, 1984
13. H. Takeda, S. Segall, P. Diament and R. Luccio, "Stable off-axis electron orbits and their radiation spectrum in a helical wiggler," Nucl Instrum Methods A237, 145 (1985)
14. S. B. Segall, S. Von Laven, M. S. Curtin and H. Takeda, "Design of a millimeter-wavelength FEL experiment employing a large-diameter beam and a quasioptical cavity," *ibid* page 234.
15. P. Diament, "Helical wiggler design with an array of uniform, small, permanent magnets," *ibid* page 381.
16. M.S. Curtin, S. B. Segall and P. Diament, "Design of a large-useful-bore permanent-magnet helical wiggler," *ibid* p 395.
17. P. Diament, "Design, optimization, and purity of permanent-magnet helical wigglers for free electron lasers," IEEE J Quantum Electron QE-21, 1094 (1985)
18. J. F. Ward and S. A. Von Laven, "Four-element linear resonators with grazing incidence mirrors for high-power FELs," *ibid* page 1108.

19. S. B. Segall, "Hybrid accelerator design for a free electron laser," IEEE Trans Nucl Sci NS-32, 3380 (1985)
20. S. B. Segall, M. S. Curtin and S. A. Von Laven, "Key issues in the design of a two-stage FEL," Proceedings of the Seventh International FEL Conference, to be published in Nucl Instrum Methods (1986)
21. M. S. Curtin, "A three-dimensional permanent-magnet helical wiggler model used to investigate off-axis orbits," *ibid*
22. S. A. Von Laven, "Results of cold testing a quasioptical cavity for a two-stage FEL," *ibid*.
23. J. F. Ward, S. A. Von Laven and S. B. Segall, "Annular reflectors for an FEL resonator," *ibid*.
24. G. J. Ramian, Proceedings of the 7th International FEL Conference, to be published in Nuclear Instrum Methods (1986).
25. W. B. Colson, "The nonlinear wave equation for higher harmonics in free electron lasers," IEEE J Quantum Electron QE-17, 1417 (1981).
26. J. A. Pasour, P. Sprangle, C. M. Tang and C. A. Kapetanacos, "High-power two-stage FEL oscillator operating in the trapped particle mode," Nucl Instrum Methods A237, 154 (1985).
27. L. Elias, Proceedings of the 7th International FEL Conference, to be published in Nucl Instrum Methods (1986).
28. Dynamitron is the name of an accelerator with a parallel-coupled voltage multiplier charging circuit manufactured by Radiation Dynamics, Inc. We will use this name in lower case to refer to all accelerators of this type.
29. M. R. Cleland and P. Farrell, "Dynamitron of the future," IEEE Trans Nucl Sci, page 227 (June 1965).

APRIL 1984

REPORTS DISTRIBUTION LIST FOR ONR PHYSICS DIVISION OFFICE
UNCLASSIFIED CONTRACTS

Director Defense Advanced Research Projects Agency Attn: Technical Library 1400 Wilson Blvd. Arlington, Virginia 22209	1 copy
Office of Naval Research Physics Division Office (Code 412) 800 North Quincy Street Arlington, Virginia 22217	2 copies
Office of Naval Research Director, Technology (Code 200) 800 North Quincy Street Arlington, Virginia 22217	1 copy
Naval Research Laboratory Department of the Navy Attn: Technical Library Washington, DC 20375	1 copy
Office of the Director of Defense Research and Engineering Information Office Library Branch The Pentagon Washington, DC 20301	1 copy
U.S. Army Research Office Box 1211 Research Triangle Park North Carolina 27709	2 copies
Defense Technical Information Center Cameron Station Alexandria, Virginia 22314	12 copies
Director, National Bureau of Standards Attn: Technical Library Washington, DC 20234	1 copy
Director U.S. Army Engineering Research and Development Laboratories Attn: Technical Documents Center Fort Belvoir, Virginia 22060	1 copy
ODDR&E Advisory Group on Electron Devices 201 Varick Street New York, New York 10014	1 copy

Air Force Office of Scientific Research 1 copy
Department of the Air Force
Bolling AFB, DC 22209

Air Force Weapons Laboratory 1 copy
Technical Library
Kirtland Air Force Base
Albuquerque, New Mexico 87117

Lawrence Livermore Laboratory 1 copy
Attn: Dr. W. F. Krupke
University of California
P.O. Box 808
Livermore, California 94550

Harry Diamond Laboratories 1 copy
Technical Library
2800 Powder Mill Road
Adelphi, Maryland 20783

Naval Air Development Center 1 copy
Attn: Technical Library
Johnsville
Warminster, Pennsylvania 18974

Naval Weapons Center 1 copy
Technical Library (Code 753)
China Lake, California 93555

Naval Underwater Systems Center 1 copy
Technical Center
New London, Connecticut 06320

Commandant of the Marine Corps 1 copy
Scientific Advisor (Code RD-1)
Washington, DC 20380

Naval Ordnance Station 1 copy
Technical Library
Indian Head, Maryland 20640

Naval Postgraduate School 1 copy
Technical Library (Code 0212)
Monterey, California 93940

Naval Missile Center 1 copy
Technical Library (Code 5632.2)
Point Mugu, California 93010

Naval Ordnance Station Technical Library Louisville, Kentucky 40214	1 copy
Commanding Officer Naval Ocean Research & Development Activity Technical Library NSTL Station, Mississippi 39529	1 copy
Naval Explosive Ordnance Disposal Facility Technical Library Indian Head, Maryland 20640	1 copy
Naval Ocean Systems Center Technical Library San Diego, California 92152	1 copy
Naval Surface Weapons Center Technical Library Silver Spring, Maryland 20910	1 copy
Naval Ship Research and Development Center Central Library (Code L42 and L43) Bethesda, Maryland 20084	1 copy
Naval Avionics Facility Technical Library Indianapolis, Indiana 46218	1 copy

END

DITIC

9 - 86